EFFECTS OF IMAGE PLANE, PATIENT POSITIONING, AND FORAMINAL ZONE ON MAGNETIC RESONANCE IMAGING MEASUREMENTS OF CANINE LUMBOSACRAL INTERVERTEBRAL FORAMINA

Claudia Zindl, Russell L. Tucker, Jelena Jovanovik, Constanza Gomez Alvarez, David Price, Noel Fitzpatrick

From Fitzpatrick Referrals Ltd (Zindl, Jovanovik, Fitzpatrick), Halfway Lane, Eashing, Godalming, Surrey GU7 2QQ, UK; Veterinary Clinical Sciences (Tucker), College of Veterinary Medicine, Washington State University, Pullman WA 99164, USA; University of Surrey, The School of Veterinary Medicine (Gomez Alvarez), Guildford, Surrey, GU2 7XH, UK; University of Cambridge, Department of Veterinary Medicine, Disease Dynamics Unit (Price), Cambridge, CB3 0ES, UK

Address corespondance and reprint requests to Noel Fitzpatrick at the above address.

Key words: lumbosacral foraminal stenosis, dogs, magnetic resonance imaging, sagittal oblique plane, hyperextended position

Running Head: LS foramina dimension in 2 planes and 2 positions

Previous Presentations or abstracts: Portions of this study were presented at the BSAVA Congress, 4-7 April 2013, Birmingham, UK; and at the WVOC Meeting, 1-8 March 2014, Breckenridge, Colorado, USA

Abstract

Degenerative lumbosacral stenosis has been suspected to have a dynamic component, especially regarding encroachment of the L7 nerve roots exiting the lumbosacral foramina. Angled cross-sectional imaging of the neuroforamina has been found improve the accuracy of the diagnosis of stenosis in humans. In this anatomic study, foraminal apertures were evaluated by magnetic resonance imaging (MRI) at the entry, middle and exit zones of the nerve roots in 30 dogs that were clinically affected by lumbosacral disease. Standard versus oblique planar orientation and neutral versus hyperextended positioning of the lumbosacral area were compared by measuring the median values for entry, middle and exit zones. The neuroforaminal area acquired using oblique plane acquisition was significantly smaller than standard parasagittal measurements. Furthermore, standard parasagittal neuroforaminal dimensions in the

hyperextended position were significantly smaller than standard parasagittal measurements in the neutral position. This statistical difference was even more pronounced for neuroforaminal dimension evaluated in the oblique plane and hyperextended position. Positioning of the dog during imaging has a significant effect on neuroforaminal dimension, corroborating the notion that spinal position may influence neural claudication in clinically affected patients. Reductions in neuroforaminal dimension are more evident on oblique planar image acquisition, suggesting that this approach may be more useful than parasagittal imaging as a tool for identifying subtle changes in L7 neuroforaminal dimensions in cases of canine lumbosacral stenosis.

Introduction

Lumbosacral disease in dogs is characterized by pain, lameness, reluctance to exercise and in case of compression of the cauda equina or L7 nerve roots exiting the lumbosacral foramina, by neurological impairment.[1] One major cause of lumbosacral disease or cauda equina syndrome is degenerative lumbosacral stenosis (DLSS).[2,3] Clinical symptoms of dogs suffering from lumbosacral stenosis can be exacerbated by exercise and certain movements,[4-8] and it is often seen in working dogs and dogs with high activity levels.[9] It is well accepted in humans that neuroforaminal impingement may be exacerbated by certain postural orientations and by axial loading of the spine.[10] In people it has been shown that walking and being in an upright position (extension of the spine and axial loading) make the symptoms worse.[11] The canine lumbosacral spine has been evaluated with flexion-extension myelography[12] and radiographic stress views.[13] In these studies it was stated that overextension of the spine was necessary to establish a diagnosis via myelography[12] and that static and dynamic components are involved in the compression and both should be evaluated.[13] Thereby it is proposed that lumbosacral stenosis and neurogenic claudication is a dynamic phenomenon and that the patient population would profit from being able to evaluate intervertebral foramina dimensions under dynamic conditions using an imaging procedure that makes measurements of the foraminae the most accurate.

Cadaveric studies in humans have shown that flexion increased the size of the foraminal area by 12% and extension decreased the area by 15%; with a 15.4% incidence of nerve root compression in the flexion group and 33.3% in the extension group.[14] Conventional recumbant MRI has been found to be inadequate for complete and thorough evaluation of the spinal column and its contents in humans.[15] Positional MRI demonstrated that minor neural compromise and positional pain score differences were significantly related to changes in foraminal size,[11] when MRI is performed in supine, erect-flexed and erect-extended positions.[16] Positional computed tomography (CT) has been found to be a feasible technique for quantifying dynamic changes in L7-S1 intervertebral foraminal morphology in dogs with lumbosacral disease[17] but a large variability in lumbosacral intervertebral foramen cross-sectional areas with a large interobserver variability has been found during lumbosacral joint extension in a cadaveric CT study.[18] Measurements of the parasagittal foramen area obtained at the entry, middle and exit zones via CT were used as a measure of success of endoscopic assisted lumbosacral foraminotomies in the dog.[19] In magnetic resonance imaging (MRI), features of DLSS are easily identified in dogs[20] and abnormal MRI findings are consistent with surgical findings.[21] Several studies have used MRI to measure different features regarding neural stenosis.[4,22] In two cadaveric dog studies it was shown that foraminal areas measured with CT[18] and MRI[23] were significantly different between flexed and extended lumbosacral positions.[18,23] The traditional imaging planes to investigate the spinal canal and the neuroforamina in magnetic resonance imaging are parasagittal, transverse (axial) and dorsal planes.[4,20,21,24,25] One study in dogs has investigated neuroforaminal dimensions and trajectories in the lumbosacral area with sagittal oblique images in computed tomography.[18] In humans, neuroforaminal dimensions are evaluated in standard parasagittal planes and image acquisition of the entry, middle and exit zones of the neuroforamina have been employed to subjectively assess L7 nerve root encroachment.[26,27] In a prospective human study it was suggested that coronal oblique lumbar MRI can precisely demonstrate nerve roots in foraminal and extraforaminal areas[28] and improve the diagnostic ability.[29,30]

Neither the effect of position of the lumbosacral spine nor the effect of a parasagittal oblique imaging plane on neuroforaminal measurements have been evaluated with magnetic resonance

imaging in dogs clinically affected by DLSS. The purpose of this study was to compare standard parasagittal foraminal measurements with those obtained in an oblique plane perpendicular to the exiting nerve root, that has been described in CT[18] in dogs. And secondly, to compare these measurements in both neutral and hyperextended positions of the lumbosacral area. Our null hypotheses were that 1) there is no difference between imaging planes and 2) there is no difference between lumbosacral position.

Materials and Methods

Animals

Thirty dogs, including agility, working and pet dogs, were prospectively recruited for this study between May 2010 and October 2012. They were all deemed to be clinically affected by lumbosacral disease and inclusion criteria were gait abnormalities, weakness or reluctance to jump, to rise or to exercise. The inclusion criteria were made selective for lumbosacral compromise, and pain on palpation of the dorsal lumbosacral area and pain on palpation of the sciatic outflow tract had to be present either as a separate expression of pain or in conjunction. All cases were examined by veterinarians at the clinic where the study was undertaken. General health of the dogs was within normal limits and other pelvic limb pathologies that could be the source of the reported clinical signs were excluded by palpation and range of motion examination of the pelvic limbs. For MRI, animals were placed under general anesthesia. They were induced with methadone (0.15-0.3mg/kg slow IV, Physeptone®, Martindale Pharmaceuticals, Harold Hill, Essex, UK), acepromazine (0.015-0.03mg/kg slow IV, Calmivet®, Vetoquinol, Lure Cedex, France) and propofol (4-6mg/kg IV, PropoFlo®, Abbott Laboratories, Maidenhead, Berkshire, UK) and maintained with isofluorane inhalation (IsoFlo®, Abbott Laboratories, Maidenhead, Berkshire, UK). After recovery from general anesthesia animals were discharged to their owners.

Magnetic resonance imaging

For MRI examination, all patients were positioned head-first in dorsal recumbency. The neutral position was obtained with legs placed in natural flexed leg position and images were acquired utilising a table integrated spinal coil. For the hyperextended position legs were extended caudally and a flex array coil was used (Fig 1). Imaging was carried out on the same MRI system (Symphony Magnetom™ 1.5T, Siemens, Erlangen, Germany) using the routine protocol for spine investigation. The protocol consisted of the following sequences: standard sagittal T2-weighted (T2W) sequence (TR 3000ms, TE 101ms, FOV 360mm, matrix 512x448) with slice thicknesses of 2.3-2.5mm and a slice gap of 10%, dorsal STIR (TR 6000ms, TE 47ms, FOC 350mm, matrix 384x270), transverse T2W (TR 3650ms, TE 99ms, FOV 200mm, matrix 394x270) and parasagittal oblique T2W (TR 2500ms, TE 105ms, FOV 220mm, matrix 320x232). The dorsal STIR and the transverse T2W sequences were not used in this specific study for data acquisition.

In hyperextended and neutral positions, and oblique and standard imaging planes, left and right foraminal apertures were evaluated for the entry, middle and exit zones of the nerve trajectory. The oblique parasagittal plane refers to a plane perpendicular to the nerve root, exiting the foramen. Fig. 2A indicates the trajectory of the L7 spinal nerve through the different zones of the neuroforamina. Parasagittal standard imaging planes are depicted to the left and parasagittal oblique to the right in the figures. The entrance zone is defined as the subarticular area medial to the pedicle, the middle zone is the area under the pars interarticularis and pedicle, and the exit zone represents the intervertebral foramen. Fig. 2B shows a T2W transverse image at the level of the lumbosacral junction with the corresponding parasagittal standard and oblique slices through the three different zones.

Foraminal areas in the three different zones were determined using the free-hand outline of the region of interest (ROI) using the integrated software image measurement tool of the MRI machine (Numaris4™ software, Siemens). The foraminal areas were measured by one investigator (JJ), a medical radiographer with extensive experience in MR imaging, in triplicate for each side in both planes and both positions. The measurements were displayed in cm^2 and averaged. Change in foraminal area was determined for neutral and hyperextended positions.

Examples of left and right entry, middle and exit zones on standard and oblique parasagittal image planes in neutral and hyperextended position are shown (Figs. 3-6).

Statistical analysis

Measurements were taken at each level of entry, middle and exit zones on both the left and right neuroforamina and were labelled as HS (hyperextended position standard plane), HO (hyperextended position oblique plane), NO (neutral position oblique plane) and NS (neutral position standard plane). A mixed-effects model was fit to all the area measurements where zone, plane, position and interactions, as well as the measurement side (L or R), were defined as fixed effects. Repeated measures were accounted for by specifying a random effect for each animal, and each zone within each animal, due to an observed interaction between zone and animal in the measured area. The response was transformed in order to ensure all modelling assumptions were satisfied. An ANOVA was performed on the final mixed-effects model to assess the significance of each of the zone, plane and position. The degrees of freedom in the ANOVA were estimated using the Satterthwaite approximation.[31] All hypothesis testing was undertaken at the 5% significance level. All analyses were conducted in the statistical software package R,[32] and the statistical tests were selected and performed by a statistician (DP) who is one of the authors.

Results

MRI images of lumbosacral foramina of thirty dogs included pure breed dogs (n=28) of nine breeds and cross breed dogs (n=2). Pure breed dogs were Border Collie (n=15), Labrador Retriever (n=4), German Shepherd Dog (n=2), Airdale Terrier (n=2), Pointer (n=1), Cocker Spaniel (n=1), Finnish Lapphund (n=1), Golden Retriever (n=1) and Lurcher (n=1). Sixteen female and 14 male dogs were part of the study. Dog ages ranged from 1.0 - 8.6 years (mean 4.7 years). Body weights ranged from 8.2 – 49.5kg (mean 23.4kg).

Four dogs (13.3%) only showed pain on palpation of the dorsal lumbosacral area (lumbosacral junction and/or spine) and four dogs (13.3%) only showed pain on palpation on the sciatic outflow tract, representing the major symptoms. Twenty-two dogs (73.4%) showed both of those signs combined. Of the 26 dogs (86.7%) showing pain on palpation of the sciatic outflow tract, eight of those dogs (30.8%) had unilateral signs. Additional clinical signs were: moderate partial to non-weight bearing lameness (n=16, 53.3%), stiffness (n=7, 23.3%), difficulties jumping or getting up (n=6, 20%), abnormal gait (n=3, 10%) crouched or haunched position (n=2, 6.7%), and weakness (n=2, 6.7%). Dogs could have more than one of the additional signs combined.

The mean and standard deviation values for foraminal area measurements are presented in Table 1 and 2, and results of the statistical comparisons for the variables are presented in Table 3. The mixed effects model indicated that no significant difference was found between right and left foramina ($p=0.1512$). The largest areas measured were the entry zone, 0.53 ± 0.09 cm^2 (mean and SD), and the exit zone, 0.55 ± 0.13 cm^2 (mean and SD). The smallest area was the middle zone with 0.42 ± 0.07 cm^2 (mean and SD). The mixed effects model indicated a significant effect of each of zone, plane, and position ($p<0.00005$). Measuring the entry or exit regions (rather than the middle region) both result in a significant increase in the measured area, on average ($p<0.00005$). Measurement in the standard plane (as opposed in the oblique plane), results in a significant increase in the mean measurement ($p<0.00005$), revealing that the neuroforaminal area acquired using oblique sagittal planes (NO, HO) was significantly smaller than measurements in the standard parasagittal plane (NS, HS), except for the hyperextended position in the middle and exit zone and the neutral position in the middle zone of the right foramina (Fig. 7, Table 1 - 3). Comparing the influences of the two different positions of the lumbosacral area, the neuroforaminal areas acquired with hyperextended positions were significantly smaller ($p<0.0001$) than measurements acquired in the neutral position - in the corresponding standard parasagittal plane (HS compared to NS) as well as the oblique parasagittal plane (HO compared to HS) (Fig. 3 - 6). Furthermore, there is a significant interaction between zone and plane. Specifically, compared to the middle zone and oblique plane, both entry and exit zones in the standard plane result in an increase in area, however

only entry is significant (p=0.0034 and p=0.7755) and the statistical difference was most pronounced for neuroforaminal dimensions evaluated in the oblique plane and hyperextended position (Fig. 3 and Fig. 5). There is a significant interaction between all of zone, plane and position (p = 0.0235, Table 3). Thus, on average, the minimal measurement area is predicted to be for the middle zone, for a dog in the hyperextended position, observed in the oblique parasagittal plane. No other lesions were found on MRI examination which might account for the reported clinical signs.

Discussion

Magnetic resonance imaging is a widely used advanced imaging modality to confirm the diagnosis of DLSS in dogs.[20] In the present study standard parasagittal MRI foraminal measurements at the level of the lumbosacral junction were compared with those obtained in a novel oblique plane perpendicular to the exiting nerve root. The mixed-effect model indicates that the neuroforaminal areas acquired using oblique sagittal planes were smaller, on average, compared to the standard plane. Furthermore, measurements in both the neutral and hyperextended positions of the lumbosacral area revealed that the neuroforaminal area was, on average, significantly smaller in the hyperextended position.

Standard parasagittal plane in MRI imaging is well established to investigate the spinal canal and the neuroforamina in humans, and one study concluded that the appropriate use of oblique section selections in human MRI can improve diagnostic capability.[29] Excellent visualisation of nerve roots and foramina with oblique imaging planes in the cervical spine was reported.[33] The relationship of nerve roots and foramina to intraforaminal structures and the boundary of the foramina can be determined including the intraforaminal fat signal.[34] Several studies investigating the diagnostic value of angled sagittal MRI in the cervical spine have been pursued in humans and oblique imaging has been found to be a more accurate test compared to conventional parasagittal planes.[35] The results of the present study reveal that the neuroforamina area acquired using oblique planar images was smaller than standard parasagittal measurements with the middle zone being the narrowest. These results are in

agreement with those of an earlier study using CT which investigated neuroforaminal dimensions and trajectories in the lumbosacral area using sagittal oblique images in dogs and found that the middle and exit zones had much smaller cross-sectional areas.[18] It was concluded in their study that oblique planes provided images in which the lumbosacral intervertebral foramen is visualized at its smallest cross section and thus the L7 nerve is visualized in true cross section. As compression of the L7 nerve within the lumbosacral intervertebral foramen may be more likely to occur at the point at which the cross-sectional area of the foramen is smallest, this imaging plane may potentially provide increased sensitivity in the diagnosis of lumbosacral foraminal stenosis and nerve root compression. Similar results were obtained in studies investigating oblique planes in the cervical spine in humans.[36] As the dimensions of the foramina are of clinical importance in the diagnosis of foraminal stenosis and radiculopathy, it is recommended in humans to add oblique MRI when the clinical exam is suggestive for radiculopathy in the cervical spine because the oblique images provide data not available from the conventional parasagittal acquisition technique. A significant correlation using MRI and CT on human cadaveric cervical spines between nerve root compression and decreased foraminal area was found which might help in the diagnosis of foraminal stenosis.[30] In another study it was concluded that angled cervical MRI provides statistically significant increase in specificity and accuracy of diagnosing foraminal stenosis, providing a clearer view of certain anatomic structures because the imaging plane is oriented perpendicular to the true course of the neural foramina and facilitates the identification of diseases, especially laterally.[35] In other studies in humans it was found that the oblique view added important information not available on the sagittal images or clarified changes seen on the axial images of cervical spine MRI.[37] The fact that diminished foraminal area is evident more pronouncedly on oblique planar image acquisition in the present study suggests that this novel plane could be used as a useful imaging tool to interrogate L7 nerve root encroachment.

Neurogenic claudication defined by intermittent pain or paresthesia in the legs in humans is brought on by walking and standing and relieved by sitting or lying.[10] In dogs with lumbosacral degenerative disease certain movements are more painful than others.[4,5-8] In the present study, foraminal apertures in the lumbosacral area revealed significant differences between

hyperextended and neutral patient positioning. Neuroforaminal dimensions in the hyperextended position were significantly smaller than in the neutral position. Thus, decreased foraminal dimensions may increase compression on neural structures embedded in the intervertebral foramen depending on lumbosacral vertebral position. This may occur when dogs are jumping over an agility course jump, into the owners' car, onto a sofa, when going up stairs, or when getting up after lying down in a curled-up position for a prolonged period, all of which are common observations in dogs affected by DLSS. Nerve root compression in the foramen occurs by facet subluxation with associated bulging of the posteroinferior portion of the ligamentum flavum and posterior/dorsal bulging of the intervertebral disc.[5] With regard to foraminal size, human studies have shown that dimensions of the neural foramina are position dependent.[11,38] Position-dependent changes in relationship of the nerve root with the adjacent disk were frequently found and change in pain score was most closely associated with foraminal changes.[11] Comparing recumbant, upright weight-bearing and dynamic-kinetic spinal imaging it was found that a greater degree of neural foraminal stenosis occurs in extension while flexion leads to lessening and resolution of narrowing.[17] Dynamic changes in L7-S1 intervertebral foraminal morphology have been found in dogs with lumbosacral disease with positional computed tomography[17], detecting a significant decrease in mean foraminal area for position in extension versus flexion. The absolute numbers of foraminal area measurement in extended position were much smaller compared to the values we retrieved in our study. This might be explained by the fact that the lumbosacral area was positioned in a extreme extended positioning in the mentioned study[17] and in a more normal position in our study. Conducting a CT study with cadaveric dogs it was found that the lumbosacral intervertebral foraminal area was smaller when the lumbosacral junction was extended, rather than flexed.[18] The significant effect of patient positioning on neuroforaminal dimension provides corroborative evidence that spinal position may influence neural claudication in clinically affected patients. In the mentioned study the middle and exit zones had much smaller cross-sectional areas compared with that of the entrance zone.[18] This is confirmed partly in our study where the middle zone has the smallest cross-sectional area in both planes and both lumbosacral positions, being more likely to be the site of compression. The exit zone in our study was smaller than the entrance zone in the hyperextended position but larger than the entrance zone in the neutral position.

This might be an indication that in the hyperextended position there is more dynamic compression of the exit zone due to anatomical change regarding positioning of ligaments and bulging of the intervertebral disc, compared to the entry zone, which is characterized by a more bony anatomy than soft tissue anatomy.

We found the same percentage of both genders to be affected by symptoms of DLSS, in contrast to other studies[39] where males were overrepresented. This might just be coincidence. Working dogs like the Huntaway have been reported to be over-represented regarding DLSS in New Zealand,[40] while the Border Collie was the main affected breed in the present study and a previous study.[39] Most dogs affected by DLSS exhibit pain and sensory dysfunction with few showing motor deficits.[41,42] Pain represents the predominant clinical sign followed by lameness, stiffness and difficulties jumping, which is also the case for the present study.[41,42] In one third of dogs in our study signs were unilateral and yet there was no significant difference of neuroforaminal dimension detected between left and right. This may point toward clinical signs not necessarily being correlated with the dimension of the intervertebral foramina measured on MRI. Other studies also observed that imaging findings do not always correlate well with clinical signs.[24] A recent study which quantified foraminal area in dogs affected by DLSS did not reveal a direct correlation between foraminal area and clinical signs.[17] Further studies are needed to investigate the relationship between clinical signs, especially dynamic movements, and MRI findings in large numbers of clinical cases. We submit that the new parasagittal oblique plane described here may be a useful diagnostic plane to diagnose foraminal stenosis more reliably, but this remains to be seen in consecutive studies.

CT is a very sensitive diagnostic imaging tool for bony changes and MRI is considered to be more sensitive for detection of soft tissue changes. The step window display facilitated discrimination of bone margins for most dogs, however also created difficulties in assessing bone margins.[17] Epidural fat surrounds the cauda equina nerve roots and provides a natural source of soft tissue contrast in normal dogs.[43] In dogs with lumbosacral stenosis, however, epidural fat is usually lost at sites of cauda equina compression. Contrast-enhanced CT has a positive-predictive value of 81% for compressive soft tissues involving the lateral recesses in dogs with lumbosacral stenosis.[44] In MRI, however, compression of the nerve roots by

protruding disc material and loss of epidural fat is easily identified.[11,20,] T1W sagittal images were found most useful in imaging the cross sectional area of the intervertebral canal and in demonstrating foraminal narrowing.[21] In the present study T2W images were chosen as the sequence to evaluate the images because the T2W images are one of the most frequently used sequences by clinicians for diagnostic purposes in a clinical setting and our objective was to provide maximal applicability to typical clinical scenarios. Together with T1W, the T2W sequence has been used in canine and human studies to diagnose foraminal stenosis.[28,42] Foraminal area with reconstructed sagittal oblique CT images was investigated by angulating standard sagittal images perpendicular to the transverse plane angle.[18] Using MRI, sagittal plane images do not need to be reconstructed as in CT and are valuable in demonstrating foraminal disc protrusion and associated foraminal stenosis with a clear advantage over CT imaging.[21] Freehand tracing around the margins of the foramen to quantify the foraminal area has been undertaken in dogs using CT images.[17,19] Because this process may be inaccurate implicating errors in positioning the cursor and in accurately defining the boundaries of the foramen, in a recent study it was attempted to improve boundary detection with modeling the soft tissue component by injecting a plastic material into the foramen of the study cadavers.[18] In the present study foraminal areas were determined using the free-hand outline of the region of interest using the epidural fat as a border for the outline of the foraminal boundaries. We accept the limitation that there is still a risk of under- or overestimation of the foraminal area and further studies including evaluation of inter- and intraobserver variability are warranted.

A second limitation of our study is that to simulate the dynamics of the lumbosacral junction the normal position was compared with the hyperextended position and not with a hyperflexed position. To investigate and demonstrate more extreme changes of foraminal dimensions under the influence of position of the lumbosacral junction, a hyperflexed position may be used in further studies. A third limitation of this study is slice thickness, which varied according to the size of the patient. We used the thickest slice size possible to minimize artifact but in some patients the slice thickness was decreased in order to relate the slices definitively to the planes of the entry, middle and exit zones. Additional limitations of the study is the lack of a group of painfree dogs with similar signalement and without any clinical signs of lumbosacral disease as

controls and the restrospective nature of the study. The inclusion criteria were made selective for lumbosacral compromise, but inherently in a retrospective study we are limited by the histories and exam findings recorded in the medical records, by several different clinicians. Besides many different nonspecific clinical signs, that can be attributed to several pelvic limb pathologies, the clinical sign all those dogs had in common was lumbosacral pain - on dorsal palpation of the lumbosacral area or pain on palpation of the sciatic outflow tract, either as a separate expression of pain or in conjunction. Despite the often nonspecific clinical signs of degenerative lumbosacral stenosis, lumbosacal pain is considered the most consistent clinical finding.[45] Lumbosacral pain can be elicited specifically by dorsal palpation of the lumbosacral area[45] and the sciatic outflow tract.[1] We considered this specific pain responses as a strong indicator for a pathology of the lumbosacral area. It is the standard of care and medical record documentation in the clinic where the study took place, that exclusion of mention of other pelvic limb lesions in the medical records indicated that the examining clinicians have excluded other etiologies. Being also part of the inherent limitation of a retrospective study, we therefore made the assumption that no other pelvic limb pathologies have been detected in the presented dogs with the assumption that the pelvic limbs were examined by widely accepted good general practice and with consistent clinical exam. There is a lack of gold standard in this study population, however using what has been published in the literature yields to us a valid form of "reference standard". The goals and results of this study are not intended to correlate the clinical signs to MRI findings. Clinical signs were intended to define inclusion criteria to create a study population with clinical signs most representative of lumbosacral pathology.

Notwithstanding the limitations of our study, we conclude that the parasagittal oblique plane may represent a potentially more accurate objective measure of L7 neuroforaminal dimensions. Furthermore, we have shown that spinal position may influence dimensions of neuroforamina as detected by MRI in clinically affected patients and that positional MRI is a feasible technique for quantifying dynamic changes in L7-S1 foraminal morphology. Authors propose that positional MRI with parasagittal oblique image acquisition should form part of any imaging interrogation of patients with clinical signs likely attributable to DLSS, particularly where conventional imaging parameters may prove inconclusive. Further application of these

techniques in larger case numbers, cohort studies, anatomical comparative studies and surgical confirmation of imaging findings will all be required to further establish applicability of our findings.

Authorship statement

Category 1

a) Conception and Design

Noel Fitzpatrick

b) Acquisition of Data

Jelena Jovanovik

c) Analysis and Interpretation of Data

Noel Fitzpatrick

Jelena Jovanovik

Claudia Zindl

David Price

Constanza Gomez-Alvarez

Russell L. Tucker

Category 2

a) Drafting the Article

Claudia Zindl

406 Russell L Tucker

407 b) Revising Article for Intellectual Content

408 Noel Fitzpatrick

409 Jelena Jovanovik

410 Claudia Zindl

411 David Price

412 Constanza Gomez-Alvarez

413 Russell L. Tucker

414

415 Category 3

416 a) Final Approval of the Completed Article

417 Noel Fitzpatrick

418 Jelena Jovanovik

419 Claudia Zindl

420 Constanza Gomez-Alvarez

421 David Price

422 Russell L.Tucker

423

424 Acknowledgement

425 The authors thank Miguel Solano and Judith Bertran for their help with graphs, David Price for
426 help with statistics and Matthew J Allen for helpful advice reviewing the manuscript.

427

428 References

429 1. Sharp NHJ, Wheeler SJ. Lumbosacral disease. In: Sharp NHJ,Wheeler SJ, editors. Small Animal
430 Spinal Disorders – Diagnosis and Surgery. Philadelphia: Elsevier; 2005. p.181-210.

431 2. Archer R, Sissener T, Connery N, Spotswood T. Asymmetric lumbosacral transitional vertebra
432 and subsequent disc protrusion in a cocker spaniel. Can Vet J 2010;51:301-304.

433 3. Oliver JE Jr, Selcer RR, Simpson S. Cauda equina compression from lumbosacral
434 malarticulation and malformation in the dog. J Am Vet Med Assoc 1987;173:207-214.

435 4. Rossi F, Seiler G, Busato A, Wacker C, Lang J. Magnetic resonance imaging of articular process
436 joint geometry and intervertebral disk degeneration in the caudal lumbar spine (L5-S1) of dogs
437 with clinical signs of cauda equina compression. Vet Radiol Ultrasound 2004;45:381-387.

438 5. Morgan JP, Bailey CS. Cauda equina syndrome in the dog: radiographical evaluation. J
439 Small Anim Pract 1990; 31:69-77.

440 6. Scharf G, Steffen F, Grünenfelder F, Morgan JP, Flückiger M. The lumbosacral junction in
441 working German Shepherd Dogs – neurological and radiological evaluation. J Vet Med A
442 Physiol Pathol Clin Med 2004; 51:27-32.

443 7. Schmid V, Lang J. Measurements on the lumbosacral junction in normal dogs and those
444 with cauda equina compression. J Small Anim Pract 1993; 34:437-442.

445 8. Wright JA. Spondylosis deformans of the lumbo-sacral joint in dogs. J Small Anim Pract
446 1980;21;45-58.

447 9. Moore GE, Burkman KD, Carter MN, Peterson MR. Causes of death or reasons for
448 euthanasia in military working dogs: 927 cases (1993-1996). J Am Vet Med Assoc
449 2001;219:209-214.

450 10. Katz JN, Dalgas M, Stucki G, Katz NP, Bayley J, Fossel AH, Chang LC, Lipson SJ. Degenerative
451 lumbar spinal stenosis - diagnostic value of the history and physical examination. Arthritis
452 Rheum 1995;38:1236-1241.

453 11. Weishaupt D, Schmid MR, Zanetti M, Boos N, Romanowski B, Kissling RO, et al.. Positional
454 MR imaging of the lumbar spine: does it demonstrate nerve root compromise not visible at
455 conventional MR imaging? Radiology 2000;215:247-253

456 12. Lang J. Flexion – extension myelography of the canine cauda equina. Vet Radiol 1988;
457 29:242-257.

458 13. Mattoon JS, Koblik PD. Quantitative survey radiographic evaluation of the lumbosacral spine
459 of normal dogs and dogs with degenerative lumbosacral stenosis. Vet Radiol Ultrasound
460 1993;34:194-206.

461 14. Inufusa A, An HS, Lim TH, Hasegawa T, Haughton VM, Nowicki BH. Anatomic changes of the
462 spinal canal and interbretebral foramen associated with flexion-extension movement. Spine
463 1996;21:2412-2420.

464 15. Jinkins JR, Dworkin JS, Green CA, Greenhalgh JF, Gianni M, Gelbien M, et al. Upright, weight-
465 bearing, dynamic-kinetic MRI of the spine pMRI/kMRI. Rivista di Neuroradiologia 2002;15:333-
466 356.

467 16. Saifuddin A. The imaging of lumbar spinal stenosis. Clinical Radiology 2000;55:581-594.

468 17. Jones JC, Davies SE, Werre SR, Shackelford KL. Effects of body position and clinical signs on
469 L7-S1 intervetrebral foraminal area and lumbosacral angle in dogs with lumbosacral disease as
470 measured via computed tomography. Am J Vet Res 2008;69:1446-1454.

471 18. Higgins BM, Cripps PJ, Baker M, Moore L, Penrose FE, McConnell JF. Effects of body position,
472 imaging plane, and observer on computed tomographic measurements of the lumbosacral
473 intervertebral foraminal area in dogs. Am J Vet Res 2011;72:905-917.

474 19. Wood BC, Lanz OI, Jones JC, Shires PK. Endoscopic-assisted lumbosacral foraminotomy in
475 the dog. Vet Surg 2004;33:221-231.

476 20. De Haan JJ, Shelton SB, Ackerman N. Magnetic resonance imaging in the diagnosis of
477 degenerative lumbosacral stenosis in four dogs. Vet Surg 1993;22:1-4.

478 21. Adams WH, Daniel GB, Pardo AD, Selcer RR. Magnetic resonance imaging of the caudal
479 lumbar and lumbosacral spine in 13 dogs (1990-1993). Vet Radiol Ultrasound 1995;36:3-13.

480 22. Da Costa R, Parent M, Partlow G, Dobson H, Homberg DL, LaMarre J. Morphologic and
481 morphometric magnetic resonance imaging features of Doberman Pinschers with and without
482 clinical signs of cervical spondylomyelopathy. Am J Vet Res 2006;67:1601-1612.

483 23. Reynolds D, Tucker RL, Fitzpatrick N. Lumbosacral foraminal ratios and areas using MRI in
484 medium-sized dogs. Vet Comp Orthop Traumatol 2014;27:333-338.

485 24. Mayhew PD, Kapatkin AS, Wortman JA, Vite CH. Association of cauda equina compression on
486 magnetic resonance images and clinical signs in dogs with degenerative lumbosacral stenosis. J
487 Am Anim Hosp Assoc 2002;38:555-562.

488 25. Ito D, Matsunaga S, Jefferey ND, Sasaki N, Nishimura R, Mochizuki M, Kasahara M, Fujiwara
489 R, Ogawa H. Prognostic value of magnetic resonance imaging in dogs with paraplegia caused by
490 thoracolumbar intervertebral disk extrusion: 77 cases (2000-2003). J Am Vet Med Assoc
491 2005;227:1454-1460.

492 26. Botwin KP, Gruber RD. Lumbar spinal stenosis: anatomy and pathogenesis. Phys Med
493 Rehabil Clin N Am 2003;14:1-15.

494 27. Attias N, Hayman A, Hipp JA, Noble P, Esses SI. Assessment of Magentic Resonance Imaging
495 in the diagnosis of lumbar spine foraminal stenosis – a surgeon's persepctive. J Spinal Disord
496 Tech 2006;19:249-256.

497 28. Heo DH, Lee MS, Sheen SH, Cho SM, Cho YJ, Oh SM. Simple oblique lumbar magnetic
498 resonance imaging technique and its diagnostic value for extraforaminal disc herniation. Spine
499 2009;34:2419-2423.

500 29. Edelman RR, Stark DD, Saini S, Ferrucci JT, Dinsmore RE, Ladd W, et al. Oblique planes of
501 section in MR imaging. Radiology 1986;159:807-810.

502 30. Sohn HM, You JW, Lee JY. The relationship between disc degeneration and morphologic
503 changes in the intervertebral foramen of the cervical spine: a cadaveric MRI and CT study. J
504 Korean Med Sci 2004;19:101-106.

505 31. Kuznetsova A, Brockhoff PB, Christensen RHB. lmerTest: Tests in linear mixed effects
506 models. R package version 2.0-30. 2016; https://CRAN.R-project.org/package=lmerTest.

507 32. R Core Team. R: A language and environment for statistical computing. 2016; RFoundation
508 for Statistical Computing, Vienna, Austria. URL https://www.R-project.org/.

509 33. Yenerich DO, Haughton VM. Oblique plane MR imaging of the cervical spine. J Comput Assist
510 Tomogr 1986;10:823-826.

511 34. Pech P. Correlative investigations of craniospinal anatomy and pathology with computed
512 tomography, magnetic resonance imaging and cryomicrotomy. Acta Radiol Suppl
513 1988;372:127-148.

514 35. Shim JH, Park CK, Lee JH, Choi JW, Lee DC, Kim DH, et al. A comparison of angled sagittal MRI
515 and conventional MRI in the diagnosis of herniated disc and stenosis in the cervical foramen.
516 Eur Spine J 2009;18:1109-1116.

517 36. Humphreys SC, An HS, Eck JC, Coppes M, Lim TH, Estkowski L. Oblique MRI as a useful
518 adjunct in evaluation of cervical foraminal impingement. J Spinal Disord 1998;11:295-299.

519 37. Modic MT, Masaryk TJ, Mulopulos GP, Bundschuh CV, Bohlman H. Cervical radiculopathy:
520 value of oblique MR imaging. Radiology 1987;163:227-231.

521 38. Wildermuth S, Zanetti M, Duewell S, Schmid MR, Romanowski B, Benini A, et al. Lumbar
522 spine: quantitative and qualitative assessment of positional (upright flexion and extension) MR
523 imaging and myelography. Radiology 1998;207:391-398.

524 39. Janssens L, Beosier Y, Daems R. Lumbosacral degenerative stenosis in the dog. Vet Comp
525 Orthop Traumatol 2009;22:486-491.

526 40. Cave NJ, Bridges JP, Cogger N, Farman RS. A survey of diseases of working farm dogs in New
527 Zealand. NZ Vet J 2009;57:305-312.

528 41. Danielsson F, Sjöström L. Surgical treatment of degenerative lumbosacral stenosis in dogs.
529 Vet Surg 1999;28:91-98.

530 42. Gödde T,Steffen F. Surgical treatment of lumbosacral foraminal stenosis using a lateral
531 approach in twenty dogs with degenerative lumbosacral stenosis. Vet Surg 2007;36:705-713.

532 43. Feeney DA, Evers P, Fletcher TF, Hardy RM, Wallace LJ. Computed tomography of the normal
533 canine lumbosacral spine: a morphologic perspective. Vet Radiol Ultrasound 1996;37:399-411.

534 44. Jones JC, Shires PK, Inzana KD, Sponenberg DP, Massicotte C, Renberg W, et al. Evaluation of
535 canine lumbosacral stenosis using intravenous contrast-enhancened computed tomography. Vet
536 Radiol Ultrasound 1999;40:108-114.

537 45. Sjöström L. Lumbosacral Disorders – Degenerative Lumbosacral Stenosis: Surgical
538 Decompression. In: Slatter D, editor. Textbook of Small Animal Surgery. New York: WB
539 Saunders; 2003. p. 1227-1243.

540

541

542

Table 1. Measured Area of Left Neuroforamina in Normal Position Standard Plane, Normal Position Oblique Plane, Hyperextended Position Standard Plane and Hyperextended Position Oblique Plane, Comparing Entry, Middle and Exit Zone (n=30)

	Entry		Middle		Exit	
	Mean (cm^2)	SD	Mean (cm^2)	SD	Mean (cm^2)	SD
HS	0.55	0.13	0.38	0.10	0.48	0.17
HO	0.43	0.10	0.34	0.07	0.42	0.13
NS	0.64	0.18	0.54	0.15	0.72	0.21
NO	0.54	0.11	0.45	0.09	0.58	0.21

NS = normal position standard plane, NO = normal position oblique plane, HS = hyperextended position standard plane, HO = hyperextended position oblique plane

Table 2. Measured Area of Right Neuroforamina in Normal Position Standard Plane, Normal Position Oblique Plane, Hyperextended Position Standard Plane and Hyperextended Position Oblique Plane, Comparing Entry, Middle and Exit Zone (n=30)

	Entry		Middle		Exit	
	Mean (cm^2)	SD	Mean (cm^2)	SD	Mean (cm^2)	SD
HS	0.53	0.14	0.37	0.09	0.46	0.16
HO	0.43	0.10	0.34	0.09	0.44	0.15
NS	0.64	0.15	0.49	0.11	0.73	0.19
NO	0.51	0.10	0.45	0.11	0.57	0.21

NS = normal position standard plane, NO = normal position oblique plane, HS = hyperextended position standard plane, HO = hyperextended position oblique plane

Table 3. Results of the ANOVA, Demonstrating the Statistical Significance of Each Variable*

	F-value	P-value
Side	2.0646	0.1512
Zone	40.0215	<0.00005
Plane	125.2637	<0.00005
Position	384.4908	<0.00005
Zone:plane	4.2470	0.0147
Zone:position	13.9338	<0.00005
Plane:position	2.8302	0.0930
Zone:plane:position	3.7742	0.0235

*The ANOVA indicates that each zone, plane, position, the two-way interaction between zone and plane, and zone and position, and the three-way interaction between zone, plane and position, all have a significant effect on the measured neuroforaminal area.

Figure legends

FIG. 1. Schematic drawings of positioning of the dogs for MRI. Neutral position was obtained with legs placed in natural flexed frog-leg position, with foam wedges placed under the distal femur/stifle area if necessary, to keep the pelvic limbs balanced. Hyperextended position was obtained with legs extended caudally to extend the hip joint, with both femora affixed parallel to each other, and elevating the lumbosacal area with sandbags.

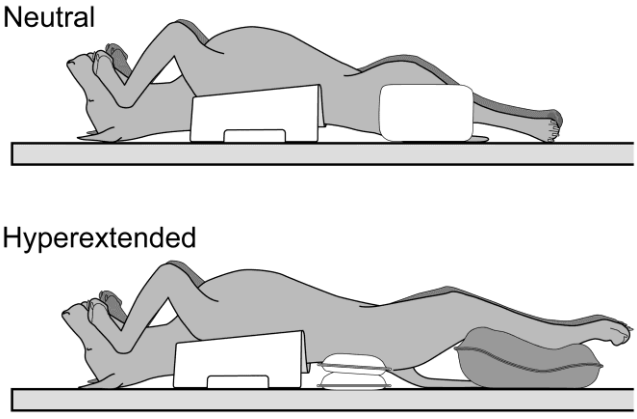

FIG. 2. Schematic drawing (A) and T2W transverse MRI image (B) at the level of the lumbosacral junction indicating the trajectory of the L7 spinal nerve through the different zones of the intervertebral neuroforamina. Parasagittal standard imaging planes are depicted to the left and

616 oblique imaging planes to the right in the drawing and the image. Entry, middle and exit zones
617 are represented from axial to abaxial by sequential arrows on image A and by lines on image B.

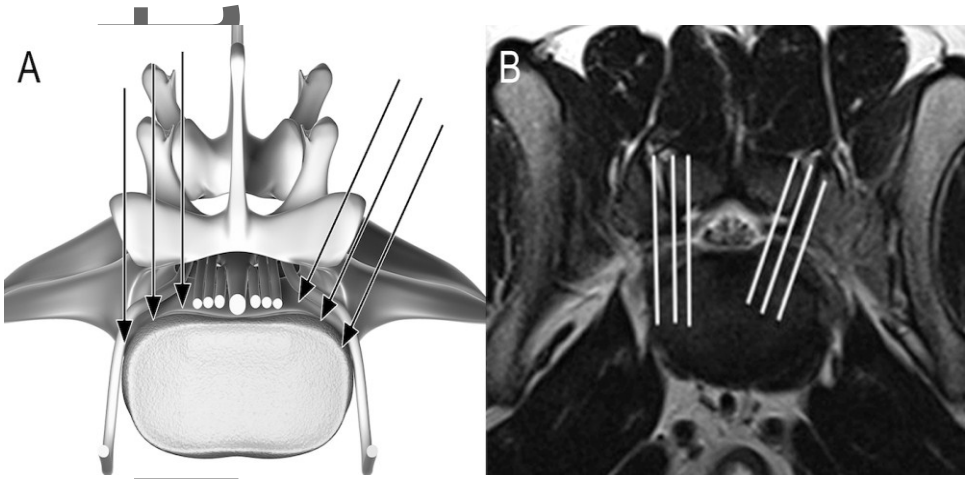

618

619 FIG. 3-6. Zone measurements as region of interest (ROI) of the foraminal aperture in the entry
620 (A), middle (B) and exit (C) zone in the parasagittal plane (T2W).
621 FIG. 3. Left standard (first row) and oblique (second row) parasagittal image planes in
622 hyperextended position of the lumbosacral area.

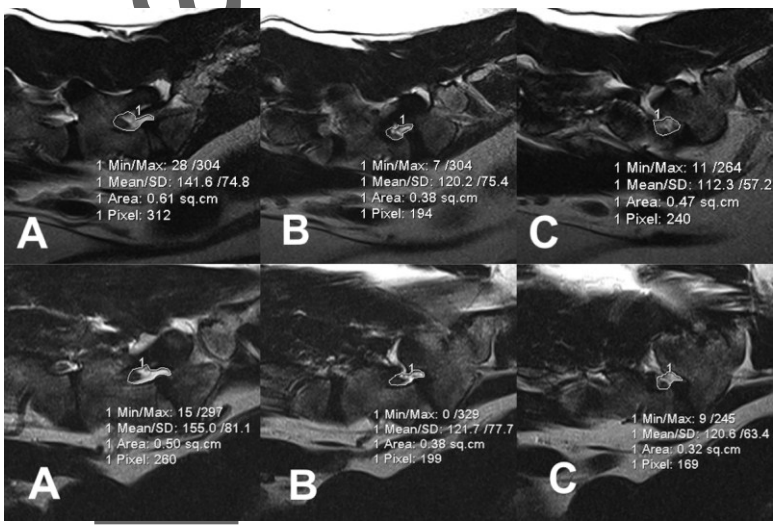

623

624

FIG. 4. Left standard (first row) and oblique (second row) parasagittal image planes in neutral position of the lumbosacral area.

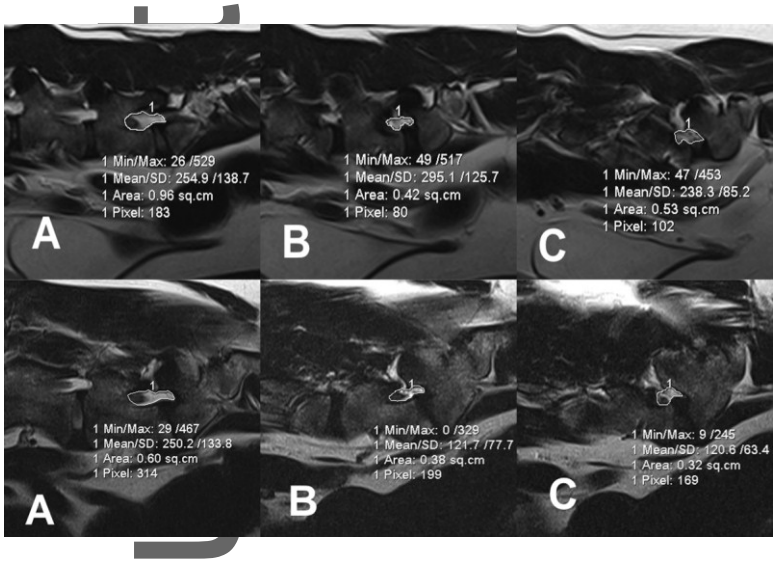

FIG. 5. Right standard (first row) and oblique (second row) parasagittal image planes in hyperextended position of the lumbosacral area.

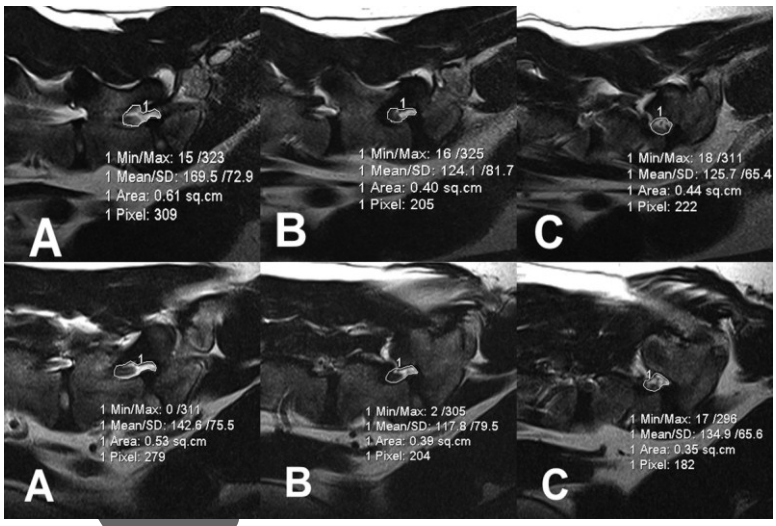

FIG. 6. Right standard (first row) and oblique (second row) parasagittal image planes in neutral position of the lumbosacral area.

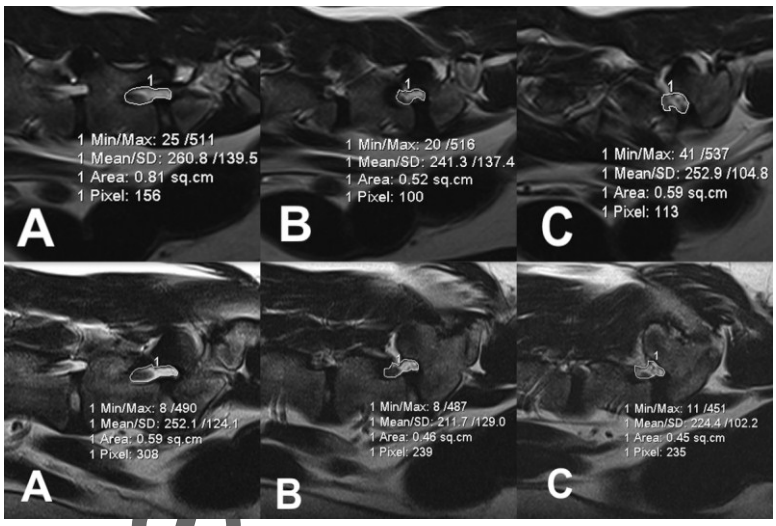

FIG. 7. Box and whisker plot of data from area measurements of the left (L) and right (R) entry, middle and exit zones of neuroforamina (cm^2) comparing two MRI views and two positions of the lumbosacral (LS) area (HS–hyperextended position standard plane, HO–hyperextended position oblique plane, NO–neutral position oblique plane, NS–neutral position standard plane).

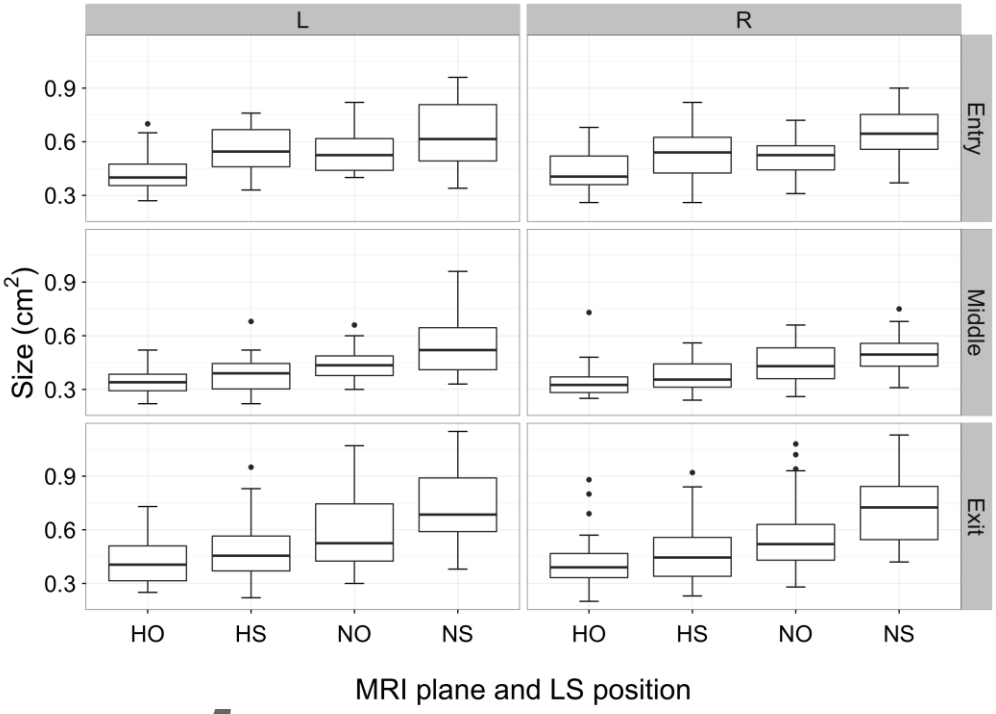

640

641

642

643

644

645

646